Superconducting Circuits and Quantum Computation

Academic and Research Staff
Professor Terry P. Orlando

Collaborators
Professor Leonid Levitov, Professor Seth Lloyd, Professor Johan E. Mooij[1], Dr. Juan J. Mazo[2], Dr. Fernando F. Falo[2], Dr. Karl Berggren[3]

Visiting Scientists and Research Affiliates
Dr. Juan Mazo[2], Professor Johan E. Mooij[1], Dr. Kenneth J. Segall, Dr. Enrique Trías

Graduate Students
Donald S. Crankshaw, Daniel Nakada, Lin Tian, Enrique Trías, Janice Lee, Bhuwan Singh

Undergraduate Students
Andrew S. Kuziemko, Michael O'Hara

Support Staff
Diane Hagopian, Scott Burris, Donna Gale

Introduction

Superconducting circuits are being used as components for quantum computing and as model systems for non-linear dynamics. Quantum computers are devices that store information on quantum variables and process that information by making those variables interact in a way that preserves quantum coherence. Typically, these variables consist of two quantum states, and the quantum device is called a quantum bit or a qubit. Superconducting quantum circuits have been proposed as qubits, in which circulating currents of opposite polarity characterize the two quantum states. Recent experiments show that these two macroscopic quantum states can be put into a superposition. In particular, microwave spectroscopy experiments indicate symmetric and anti-symmetric quantum superpositions of macroscopic states.

The goal of the present research is to use superconducting quantum circuits to perform the measurement process, and also to model the sources of decoherence, and to develop scalable algorithms. A particularly promising feature of using superconducting technology is the potential of developing high-speed, on-chip control circuitry with classical, high-speed superconducting electronics. The picosecond time scales of this electronics means that the superconducting qubits scan be controlled rapidly on the time scale that the qubits remain phase-coherent.

Superconducting circuits are also model systems for collections of coupled classical non-linear oscillators. Recently, we have demonstrated a ratchet potential using arrays of Josephson junctions as well as the existence of a novel non-linear mode, known as a discrete breather. In addition to their classical behavior, as the circuits are made smaller and with less damping, these non-linear circuits will go from the classical to the quantum regime. In this way, we can study the classical-to-quantum transition of non-linear systems.

---

[1]Delft University of Technology, The Netherlands
[2]University of Saragoza, Spain
[3]M.I.T. Lincoln Laboratory

1. Superconducting Persistent Current Qubits

Sponsors
NSA and ARDA under ARO
Grant DAAG55-98-1-0369

Project Staff
Lin Tian, Donald S. Crankshaw, Daniel Nakada, Caspar H. van der Wal[1], Professor Leonid Levitov, Professor Seth Lloyd, Professor Johan E. Mooij[1], Professor Kees Harmans[1], Alexander C.J. ter Haar[1], Frank K. Wilhelm[1], Raymond N. Schouten[1], Professor Terry P. Orlando

Quantum computers are devices that store information on quantum variables such as spin, photons, and atoms, and process that information by making those variables interact in a way that preserves quantum coherence. Typically, these variables consist of two-state quantum systems called quantum bits or 'qubits'. To perform a quantum computation, one must be able to prepare qubits in a desired initial state, coherently manipulate superpositions of a qubit's two states, couple qubits together, measure their state, and keep them relatively free from interactions that induce noise and decoherence.

We have designed a superconducting qubit that has circulating currents of opposite sign as its two states. The circuit consists of three nano-scale aluminum Josephson junctions connected in a superconducting loop and controlled by magnetic fields.

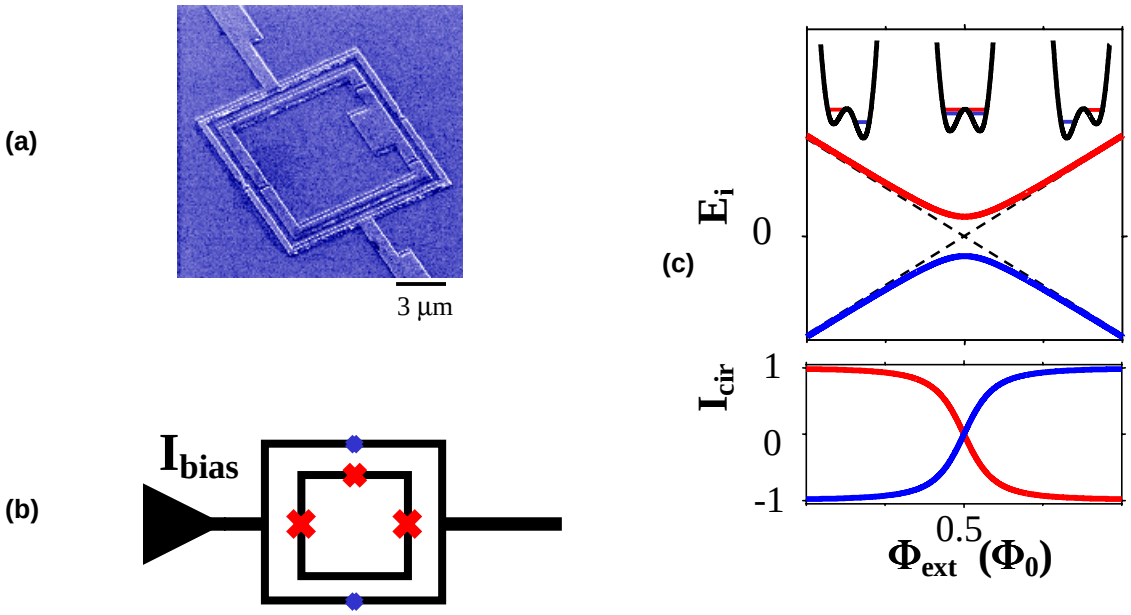

FIGURE 1. (a) SEM image of the persistent current qubit (inner loop) surrounded by the measuring dc SQUID. (b) a schematic of the qubit and measuring SQUID, the x's mark the Josephson junctions. (c) The energy levels for the ground state (blue line) and the first excited state of the qubit versus applied flux. The double well potentials are shown schematically above. The lower graph shows the circulating current in the qubit for both states as a function of applied flux. The units of flux are given in terms of the flux quantum.

[1]Delft University of Technology, The Netherlands

Figure 1a shows a SEM image of the persistent current qubit (inner loop) and the measuring dc SQUID (outer) loop. The Josephson junctions appear as small "breaks" in the image. A schematic of the qubit and the measuring circuit is shown in Figure 1b, where the Josephson junctions are denoted by x's. The qubit loop is $5 \times 5\ \mu m^2$ with aluminum-oxide tunnel junctions, microfabricated at the TU Delft, by a shadow evaporation technique. (This is in contrast to the samples fabricated at MIT's Lincoln Laboratory that are made in niobium by photolithographic techniques on a trilayer of niobium-aluminum oxide-niobium wafer.) The capacitance of the junction is estimated to be about 3 fF and the ratio of the Josephson energy to the charging energy is about 40. The inductances of the inner qubit loop and the outer measuring loop are about 11 and 16 pH respectively, with a 7 pH mutual inductive coupling.

The energy levels of the ground state (blue line) and the first excited state (red line) are shown in Figure 1c near the applied magnetic field of 0.5 Φ_0 in the qubit loop. Classically the Josephson energy of the two states would be degenerate at this bias magnetic field and increase and decrease linearly from this bias field, as shown by the dotted line. Since the slope of the *E* versus magnetic field is the circulating current, we see that these two classical states have opposite circulating currents. However, quantum mechanically, the charging energy couples these two states and results in a energy level repulsion at $\Phi_{ext} = 0.5\ \Phi_0$, so that there the system is in a linear superposition of the currents flowing in opposite directions. As the applied field is changed from below $\Phi_{ext} = 0.5\ \Phi_0$ to above, we see that the circulating current goes from negative, to zero at $\Phi_{ext} = 0.5\ \Phi_0$, to positive as shown in the lower graph of Figure 1c. This flux can be measured by the sensitive flux meter provided by the dc SQUID.

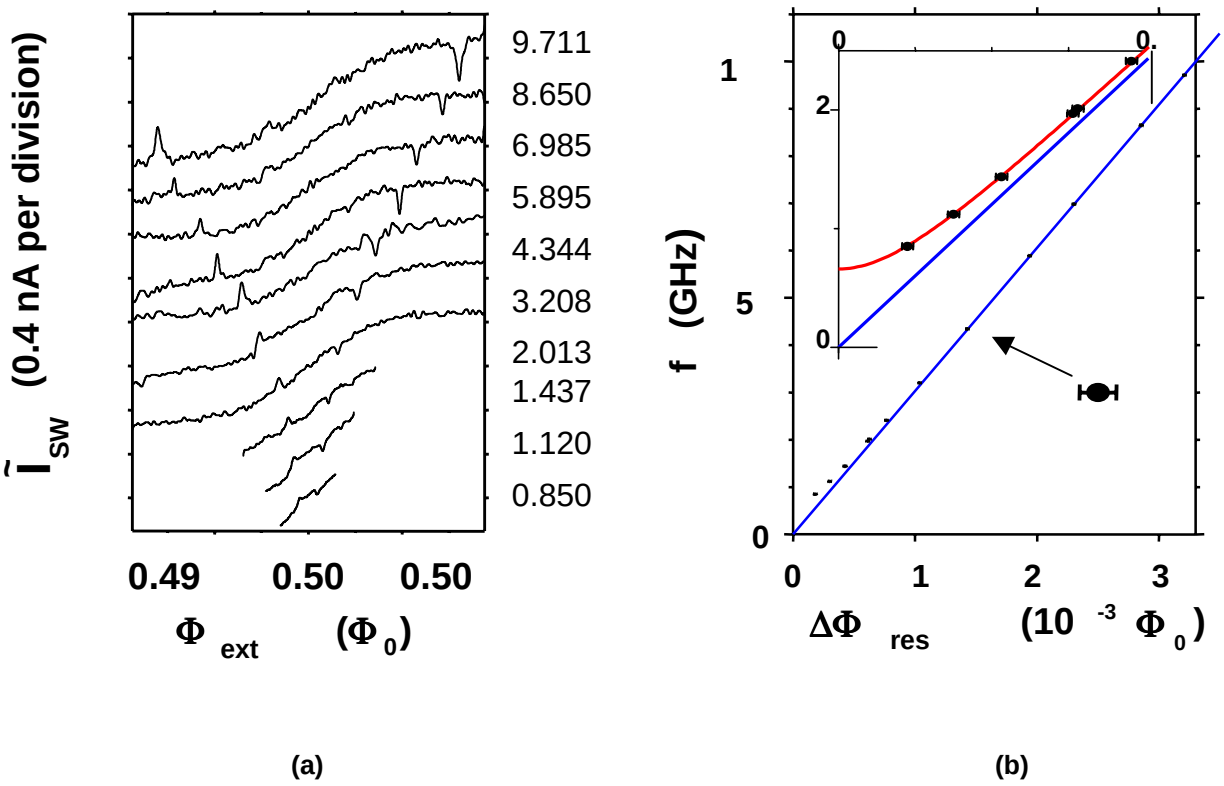

FIGURE 2. (a) The circulating current as inferred from the dc SQUID measurements for various applied microwave frequencies. The curves are offset for clarity. (b) Half the distance in Φ_{ext} measured between the resonant peaks and the dips at different frequencies *f*. The inset shows the low frequency data points. The blue line is a linear fit through the high frequency points and zero. The red line is a fit of the quantum theory.

Figure 2a shows the circulating current as inferred from the dc SQUID measurements for various applied microwave frequencies. The curves are offset for clarity, and each curve shows the expected change from negative circulating current at low applied flux, to zero at half a flux quantum, and then to positive current at higher flux. This clearly shows that the qubit has the change in flux profile expected of the ground state. When microwaves are applied at the energy difference matching the difference between the ground state and the first excited state, then a transition is induced from the ground state to the first excited state. These are shown by the resonant-like structures in each curve. A plot of the distance in Φ_{ext} at the resonance from $\Phi_{ext} = 0.5\ \Phi_0$ is shown in the figure on the left. Quantum mechanically the energy is expected to follow the form

$$\Delta E = \sqrt{\left[2I_p\left(\Phi_{ext} - 0.5\Phi_0\right)\right]^2 + \left(2V\right)^2}$$

where I_p is the circulating current and V is the tunneling matrix element between the two circulating current states at $\Phi_{ext} = 0.5\ \Phi_0$. The inset shows a fit to the curve which gives an energy gap of about 600 MHz and a circulating current of about 500 nA as expected. These results are among the first experimental verification of the superposition of macroscopic circulating current states.

2. Integrated Superconducting Device Technology for Qubit Control

Sponsors
NSA and ARDA under ARO
Grant DAAG55-98-1-0369
Lincoln Laboratory New Technology Initiative Program

Project Staff
Daniel Nakada, Michael O'Hara, Dr. Karl Berggren[1], Terence Weir[1], Earle Macedo[1], Richard Slattery[1], Professor Terry Orlando

Quantum computing requires the time-dependent control and readout of qubit couplings. Critical to the project of quantum computing is therefore the integration of quantum devices with conventional superconducting digital and analog electronics that will be used to provide classical circuitry for control and readout functions of the quantum computer. The "classical" and "quantum" devices can be integrated using inductive coupling between chips bonded by a flip-chip process. There exists a classical electronics family based on superconductive electronics-Single Flux Quantum (SFQ) logic – having the capability of operating well above 100GHz clock speeds. Such devices can be used to execute many control operations before substantial decoherence occurs in the persistent current qubit – a feature that could benefit other solid-state qubit technologies with long coherence times. The flip-chip process is not limited to the field of quantum computing but has applications in any technology that would benefit from SFQ electronics.

[1]MIT Lincoln Laboratory

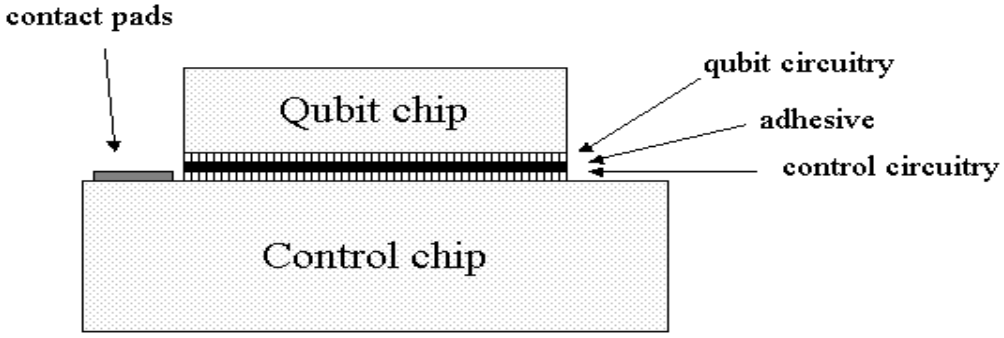

FIGURE 3. Cross section of a packaged chip. For our initial experiment, the "qubit" chip contained the transformer loop while the "control chip" included the control line and dc SQUID, coupled together via the transformer loop.

We have designed experiments to couple current magnetically from a carrier chip, onto a flipped chip (Figure 3), and back onto a different area of the carrier chip where the resulting magnetic field was sensed with a dc SQUID. The flipped chip lies less than 2μm above the carrier chip with less than 2μm of linear misalignment. The magnetic coupling between the current line and dc SQUID was enhanced due to the presence of a transformer loop on the flipped chip. To show this, we compared the effective mutual inductance between the control current and the dc SQUID with and without the presence of the flipped-chip. For quantum computing implementation, the flipped chip would carry the qubits while the carrier chip will contain the control and readout circuitry for determining the state of the qubit.

Our next step will be to design SFQ circuitry for manipulation and control of the superposition states of the persistent current qubit. Using an on-chip oscillator, we propose using timed microwave pulses to excite the qubit from the ground state to the first excited state. We also plan to increase coupling between the carrier chip and flip-chip by improving alignment as well as decreasing the chip-to-chip distance. We hope our efforts demonstrating the control of a single qubit will be an initial step towards a full-scale quantum computer.

3. Resonant Cancellation of Off-resonant Transitions in a Multilevel Qubit

Sponsors
NSA and ARDA under ARO
Grant DAAG55-98-1-0369

Project Staff
Lin Tian, Professor Seth Lloyd, Professor Johan E. Mooij[1], Professor Frank K. Wilhelm[1], Professor Terry Orlando

Off-resonant effects are a significant source of error in quantum computation. Physical qubits are not ideal two level systems, but have many higher levels that are irrelevant for the qubit operation. The off-resonant transitions to the higher levels of a qubit during a gate operation is a particularly important form of intrinsic qubit error. Numerical simulation shows that this effect can introduce an error amplitude as

[1] Delft University of Technology, The Netherlands

high as 1% in the superconducting persistent current qubit, which is significantly higher than the noise from environmental fluctuations of the qubit.

To correct this error and accomplish quantum computation, we study the effect of the higher levels on qubit dynamics during qubit operation by a group theory approach. We prove that the errors can be completely avoided by applying a time varying operation Hamiltonian. The transformations on an N-level quantum system are described by the N^2 dimensional compact Lie group $U(N)$. By applying controllable pulses of Hamiltonian H_l, with $[H_0, H_l]$, any transformation in $U(N)$ can be reached within N^2 number of pulses. This shows that the transformation on a given quantum system can be restricted to the lowest two levels with time varying pumping.

This study was then generalized to the qubit error resulting from the interaction between different qubits. Qubit interaction is necessary for operations such as a CNOT gate that is necessary for the universal set of quantum gates of quantum computation. But qubit interaction also introduces operational errors by additional transition matrix elements during gate operations. By mapping the interacting qubits as a multilevel quantum system with higher levels, the same method can be applied to correct the errors in the coupled qubit system.

By extending the idea of dynamic pulse control by Viola and Lloyd, we designed a pulse sequence that cancels the leakage to the higher levels to arbitrary accuracy with $O(N)$ number of pulses, N being the number of higher levels. This approach exploits "bang-bang" control techniques where the dynamics of the qubit and its environment is manipulated by fast pulses that flip the qubit state. With the influence of the environment being averaged out, the qubit evolves in the error-free subspace. This method relies on the ability to apply the pulses rapidly compared with the correlation time of the environment. This is an open loop control method.

In the proposed method, we apply resonant pulses between different eigen-levels to cancel the unwanted off-resonant transitions to the higher levels. All the pulses applied have the same time duration. By adjusting the amplitudes and phases of the pulses, the leakage to higher levels can be completely suppressed at the end of the operation. Since all the pulses in this sequence have the same pulse length, they can be combined into one pulse with slightly different parameters. This method for protecting quantum information is complementary to quantum error correcting codes and the `bang-bang' technique mentioned above. Like the bang-bang method, it has the advantage that it does not require extra qubits to enact. The proposed method protects against a different class of errors from those corrected by the methods of Viola, however. Dynamic pulse control can be used in conjunction with quantum error correcting codes and bang-bang decoupling methods.

4. Relaxation of a Coherent Quantum System During Premeasurement Entanglement

Sponsors
NSA and ARDA under ARO
Grant DAAG55-98-1-0369

Project Staff
Lin Tian, Professor Seth Lloyd, Professor Johan E. Mooij[1], Frank K. Wilhelm[1], Caspar H. van der Wal[1], Professor Leonid Levitov, Professor Terry Orlando

Recent experiments on superconducting loops have demonstrated macroscopic quantum effects. These experiments used a dc SQUID to measure the magnetic flux generated by the persistent currents of the macroscopic quantum states. Due to the inductive interaction between the qubit and the SQUID, the relaxation and dephasing of the qubit are limited by the entanglement with the measurement device as well as its coupling to the solid-state environment. We studied the effect of the meter (SQUID)

[1] Delft University of Technology, The Netherlands

environmental spectrum density on the qubit dynamics within the spin-boson formalism. The results can be applied to optimizing the measurement circuit for the best measurement efficiency.

As the ramping current to the dc SQUID increases, the interaction between the qubit and the dc SQUID entangles the qubit state and the SQUID state. This entanglement brings indirect interaction between the qubit and the SQUID environment and introduces additional noise to the qubit. As this interaction does not commute with the qubit Hamiltonian, it influences the qubit dynamics non-trivially. The effective spectrum density seen by the qubit is renormalized due to the presence of the meter degrees of freedom and has a different shape from the spectrum density seen by the meter.

The qubit dynamics can be described within the master equation approach when the interaction with the environment is weak. From this approach the relaxation and decoherence of the qubit, also called the transversal relaxation and the longitudinal relaxation rates, are described by the spectrum density of the environment. As the inductive interaction induces a σ_z interaction between the qubit and SQUID environment, the qubit Hamiltonian H_0 has non-commuting σ_x component with the σ_z interaction, a transversal interaction that flips the qubit and eventually relaxes the it in the qubit eigen basis is created.

This transversal interaction depends on both the tunneling between the two localized qubit states and the inductance coupling quadratically. With the renormalized spectrum density, the qubit is damped strongly by the SQUID environment. This effect prevents the measurement of the coherent oscillation between the macroscopic states with the current experimental setup.

Our study also suggests that by engineering the measurement circuit, we can optimize the spectrum density seen by the qubit and minimize the relaxation of the qubit due to various environmental fluctuations. Within the theoretical framework, various designs can be analyzed and compared.

5. Inductance Effects in the Persistent Current Qubit

Sponsors
NSA and ARDA under ARO
Grant DAAG55-98-1-0369

Project Staff
Donald S. Crankshaw, Professor Terry Orlando

In the original description of the persistent current qubit, the inductance was neglected in the energy level calculations. The effects of the small inductance in the PC qubit can be included by using a perturbative approach. This technique simplifies the numerical calculations by reducing the dimensionality of the Schrödinger equation that must be solved. Consider a circuit with *b* branches, each with a Josephson junction, connected at *n* nodes to form *m* meshes (loops). In general, the dimensionality of the Schrödinger equation for such a circuit is $b=n+m-1$. If the inductance of each mesh is small so that $\beta_L<<1$, the energy levels can be calculated by ignoring the inductances (i.e., setting $\beta_L=0$). The dimensionality of the resulting Schrödinger equation is the number of independent nodes $n-1 < b$. Moreover, we find that the Hamiltonian can be written in the form

$$H_b = H_n(\Theta_n) + H_m(I_m) + \Delta H(\langle\Theta_n\rangle, \langle I_m\rangle) . \quad (2)$$

The full Hamiltonian, H_b, of *b* variables is written in terms of three Hamiltonians: the first, $H_n(\beta_n)$, is of the form of what one would write with $\beta_L=0$, and has $n-1$ node variables β_n. $H_n(\beta_n)$ is periodic in each of these variables. The second, $H_m(I_m)$, is of the form of a simple harmonic oscillator of the *m* mesh (circulating) current variables. The last term is a correction term that can often be neglected in calculating the energy levels. If we can separate the Hamiltonian this way, the mesh Hamiltonian and the correction term are easily solved analytically (since one is a simple harmonic oscillator and the other is calculated from the

expectation values of the other Hamiltonians' variables), leaving only the node Hamiltonian, which has a lower dimensionality than the branch Hamiltonian and is periodic in all its variables. This is solved numerically. (This reduces the computational time of $O(N^b)$ for H_b to $O(N^{n-1})$, $O(m)$, and $O(n\mathrm{N}+m)$ for the terms H_n, H_m, and ΔH respectively, where N is the number of discretized elements of the quantum phase variables.)

When the qubit is modeled in a way to facilitate this derivation (see Figure 4), it reduces to the simplified equation

$$E = E_q(f) + (n+\tfrac{1}{2})\hbar\omega_0 - \tfrac{1}{2}L_m I_c^2\left(\frac{\alpha}{1+2\alpha}\right)^2\left(\left\langle \sin\left(2\tilde{\Theta}_m + 2\pi f\right)\right\rangle - \left\langle 2\cos\Theta_p \sin\tilde{\Theta}_m\right\rangle\right)^2. \quad (3)$$

The first term is the original, zero inductance solution to the qubit energy, the second term is the harmonic oscillator of the circulating current variables, and the final term is the correction term. The result for a realistic value of the qubit inductance is shown in Figure 4, which indicates that the deviation from the zero inductance solution in negligible.

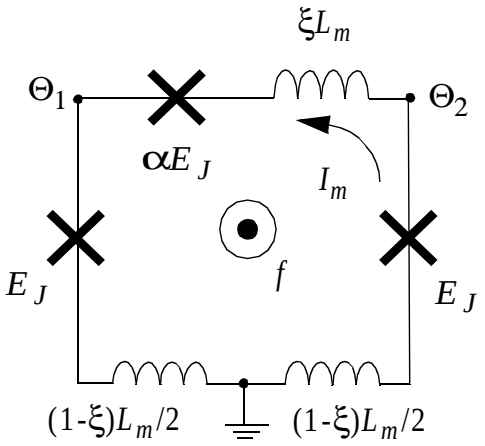

(a)

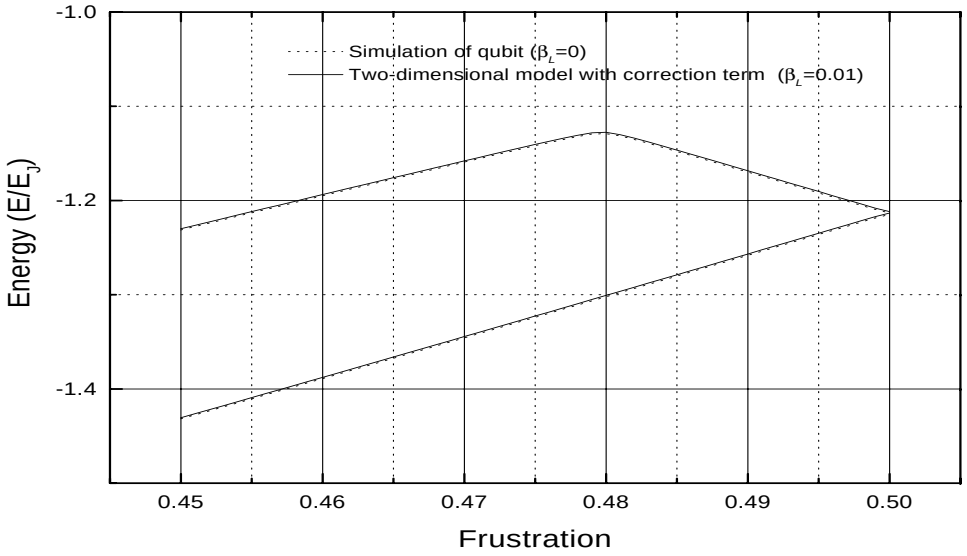

(b)

FIGURE 4. (a) The circuit used to derive the PC qubit Hamiltonian with inductance. (b) A comparison of PC qubit with and without a small inductance. The β_L was chosen to reflect the estimated geometric inductance of the fabricated qubit. The region shown in the diagram is that used for quantum computation.

6. Engineering Josephson Oscillators

Sponsors
National Science Foundation
Grant DMR 9988832
NSA and ARDA under ARO
Grant DAAG55-98-1-0369

Project Staff
Donald S. Crankshaw, Dr. Enrique Trías, Professor Terry Orlando

As the telecommunications revolution pushes for denser utilization of the spectrum, there is a need to develop inexpensive sources and detectors that operate in the 100 GHz to several THz range. It is precisely in this range that Josephson junctions provide an almost ideal solid state, current controllable source.

Arrays of junctions provide for relatively large power but due to non-linearities they can exhibit diverse complex spatiotemporal patterns. Experiments, simulations, and analysis were performed on a broad range of discrete arrays of Josephson-junction oscillators in order to understand their ability to produce coherent radiation. Networks ranging from single square and triangular plaquettes to one- and two-dimensional arrays were studied. In each array, the junctions are identical, and the arrays are driven by dc bias currents. Although few analytical results are known for these systems, we study the technically interesting solutions which can be represented as traveling waves. It is in this mode that the devices can be used as submillimeter wave sources.

Using the mathematical technique of harmonic balance it is possible to create an equivalent linear circuit of a Josephson network that is operating in a traveling wave mode. Though the non-linearity of the system allows for mixing of all the harmonics, in underdamped systems we find that the first harmonic is orders of magnitude stronger than the rest. In general, any variable can be decomposed in terms of its dc and ac spectrum. If we further restrict the ac component to a single frequency as suggested by our simulations, then the branch current and voltage across a junction can be written as:

$$\begin{aligned} I &= I_{DC} + i_{ac} e^{j\omega t} \\ V &= V_{DC} + v_{ac} e^{j\omega t} \\ I_c &= e^{jk}, \\ I_M &= \frac{v_{ac}}{j\omega} \frac{e^{-jk}}{2}. \end{aligned} \tag{3}$$

Our equivalent circuit then consists of a dc bias circuit and a mixing circuit that creates the first harmonic. Figure 5 depicts the equivalent circuit. Here k represents the phase difference between the first harmonic and the rotating part of the Josephson oscillation, and the mixing current, I_M, represents the nonlinear interaction between them. This equivalent circuit makes it possible to use powerful circuit theoretic tools to understand a Josephson network.

This model has been used to design a matched load detector. A Josephson junction can be used to detect and measure power, and designing a detector to match the impedance of an array allows us to measure the power produced by the array. As shown in Figure 6, experiments measuring the power which an array of 54 overdamped junctions delivers to an impedance match load attest to the usefulness of our model, giving a strong qualitative correlation between the predicted and measured power for varying magnetic flux (measured in units of frustration, the number of flux quantum per unit cell).

Currently, much of our oscillator work is designed to drive quantum circuits, such as the qubit and the quantum ratchet. The oscillators designed for this work are less focused on maximum power than minimum decoherence, meaning that designs may benefit from deliberately unmatched impedances. The exacting requirements of this application further test the accuracy of our model in a challenging regime.

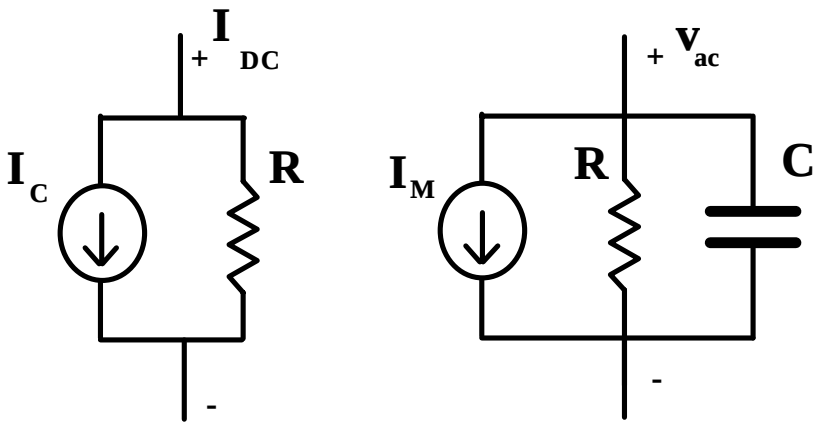

FIGURE 5. Equivalent circuit for a Josephson junction in a voltage state and with a single harmonic. Non-linearity is captured by I_M which is a mixing current that describes the interaction between the rotating Josephson phase and its first harmonic.

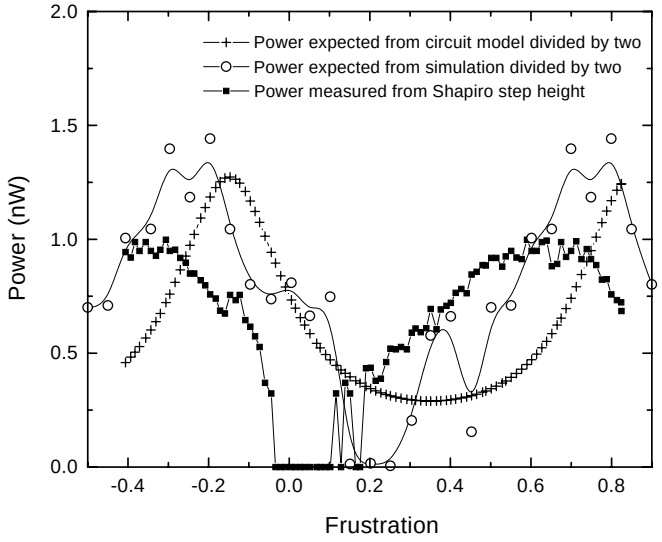

FIGURE 6. The power produced by the array, experimental measurements compared to nonlinear simulation and linear circuit model predictions. The array is biased at V_{arr} = 0.1035 mV.

7. Vortex Ratchets

Sponsorship
National Science Foundation
Grant DMR 9988832

Project Staff
Dr. Kenneth Segall, Dr. Enrique Trías, Dr. Juan J. Mazo, Dr. Fernando F. Falo, Professor Terry Orlando

Disorder and noise are not always undesirable in physical systems. An interesting, almost counterintuitive result is obtained when one studies the transport of a Brownian particle in an asymmetric potential. Under certain circumstances these systems can display net particle transport, despite the absence of any gradients. Originally proposed by Feynman, these systems with a so-called "ratchet" potential display a unique variety of behavior and suggest several possible applications. Ratchets were initially proposed as a model for molecular motors in biological organisms, and more recently as a model system in studying dissipative and stochastic processes in nanoscale devices. Ratchets have also been proposed as voltage and current rectifiers in cryogenic circuits, as devices for phase separation, and for a method of flux cleaning in superconducting thin films. A ratchet mechanism has also been proposed as a method to prevent mound formation in epitaxial film growth.

A ratchet potential is a periodic potential which lacks reflection symmetry (in 1D $V(x)$ not equal to $V(-x)$, see Figure 7). A consequence of this symmetry breaking is the possibility of rectifying non-thermal or time correlated fluctuations. This can be understood intuitively. In Figure 9, it takes a smaller dc driving force to move a particle from a well to the right than to the left. In other words, the spatial symmetry of the dc force is broken. When driven out of equilibrium, such as under an ac drive or time-correlated noise, particles show net directional motion in the smallest slope direction. This effect can be studied theoretically and used in devices in which selection of particle motion is desired.

In Josephson-junction parallel arrays, kinks (or vortices) behave as particles in which this idea of Brownian rectification can apply. The applied current is the driving force. The potential is determined by the size and geometry of the junctions in the array. If the potential has the form of a ratchet potential, then the current needed to move the kink in one direction is different than the current to move it in the opposite direction.

We have designed, fabricated and measured circular parallel arrays (rings) in order to study the motion of kinks through a ratchet potential. Figure 8 shows typical IV's for the different measured rings. Figure 8 (a) is for a regular ring with a single trapped vortex. The IV is symmetric with respect to applied current direction. As the current is increased from zero the voltage remains at zero, which implies that the vortex is pinned. As the current increases beyond the depinning value, a voltage is developed, implying that the kink is now moving around the ring. At higher currents voltage steps develop, which are resonances between the moving vortex and the electromagnetic modes of the ring. Figure 8 (b) is a ring where the junctions have alternating critical currents. We again see that the IV is symmetric with respect to current direction and that there are voltage steps. Figure 8 (c) is a ring with alternating areas. The characteristics are similar to that of ring 8 (b). Since for these three rings the depinning current is the same in the positive and negative direction, we can infer that the kink is traveling in a symmetric pinning potential. This was expected from our models.

Figure 8 (d) shows an IV for the ring with both alternating critical currents and areas. The IV of this ring is qualitatively different from the other rings. We see that the depinning current in the positive direction is ~65% of the depinning current in the negative direction. Such a difference implies that the kink is traveling in a ratchet potential. We also note that there are different voltage steps excited in the up and down direction.

We have measured the depinning of trapped kinks in this ratchet potential and compared it with the other circular arrays. We find experimentally and numerically that the depinning current depends on the direction of the applied current only in the ratchet ring. We also find other properties of the depinning current versus applied field, such as a long period and a lack of reflection symmetry, which we can explain analytically. In future experiments we plan to drive the system out of equilibrium with an ac current, and look for the directed transport of the kinks. Such experiments will begin to verify the essential predictions of ratchet behavior.

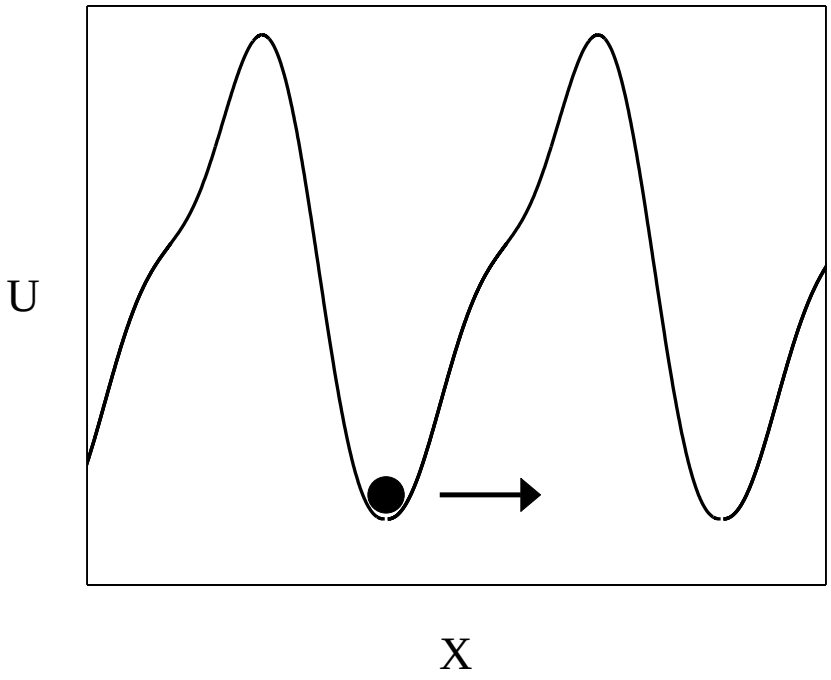

FIGURE 7. Example of a ratchet potential. The particle sitting on the well requires less force to move through the first peak to the right than to move to the left. Therefore, there is a preferred direction of motion.

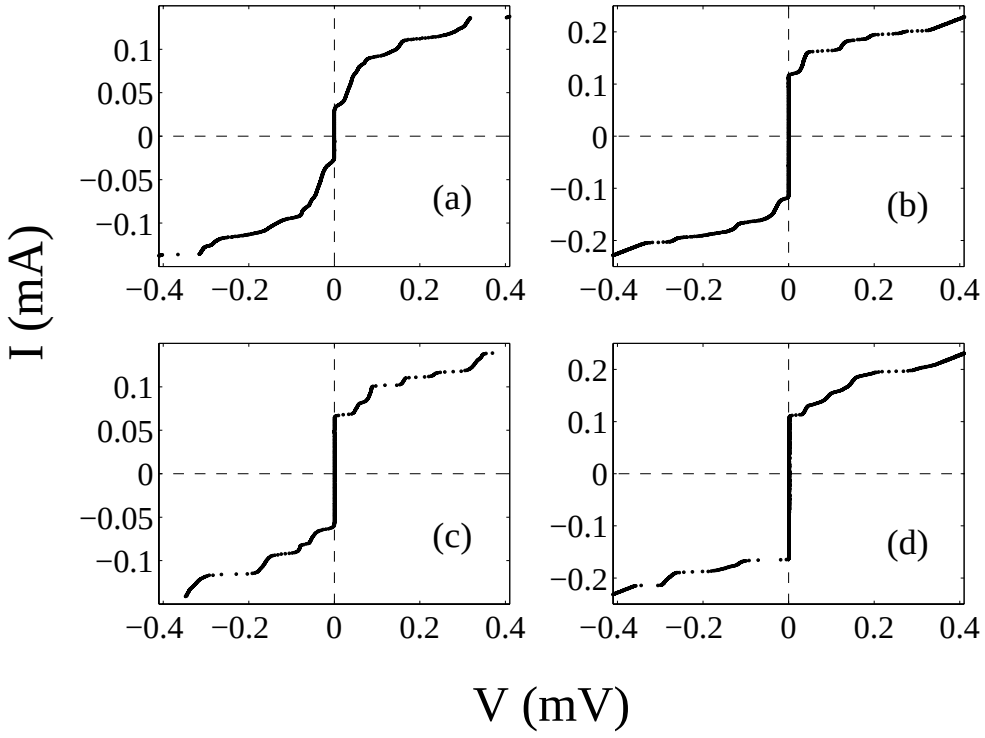

FIGURE 8. Sample IV curves for the four measured rings. Rings (a), (b), and (c) have symmetric IV's as the current is swept in the positive and negative direction. The measurements correspond to *M*=1. Ring (d) is the ratchet ring as can be seen from the difference in the depinning current in the positive and negative direction.

8. Discrete Breathers in Josephson Arrays

Sponsors
National Science Foundation
Grant DMR 9988832
Fulbright/MEC Fellowship

Project Staff
Dr. Kenneth Segall, Dr. Juan J. Mazo, Dr. Enrique Trías, Dr. Alexander Brinkman, Professor Terry Orlando

Linear models of crystals have been instrumental in developing a physical understanding of the solid state. Many thermodynamic properties, transport properties and photon interaction properties of a crystal can be understood by modeling it as an atomic lattice with fixed harmonic interactions. Certain properties of solids, however, cannot be understood in this model. In describing thermal expansion, for example, one often finds that the elastic constants of the atomic interactions depend on temperature or the volume so as to make their interaction non-linear. The usual approach in treating these so-called anharmonic effects is to use a generalized Taylor expansion for the lattice interaction that includes more than just the harmonic term.

Until quite recently anharmonic effects were studied as perturbations to the fully solvable harmonic model, which uses extended plane waves as its basis. Then it was discovered that the non-linearity may lead to *localized* vibrations in the lattice that are not adequately described by a plane wave approach. These intrinsically localized modes have been termed discrete breathers because their amplitudes oscillate around a few sites in the lattice and do not depend on impurities for their localization. Discrete breathers have been shown to be generic modes in many non-linear lattices, hence they have been the object of great theoretical and numerical attention. However, until recent work by our group (and one other) they had yet to be detected in any experiment.

We have designed experiments to detect localized modes (discrete breathers) in Josephson-junction anisotropic ladder arrays biased by dc external currents. We have done numerical simulations of the dynamics of such ladders at experimentally accessible values of the parameters of the array. We have also developed a method for exciting a breather in the array and detected their existence experimentally. We distinguish between two families of solutions which present different voltage patterns in the array. Both types are robust to random fluctuations and exist over a range of parameters values and array sizes.

Our anisotropic ladders (see Figure 9) contain junctions of two different critical currents: I_{ch} for the horizontal junctions and I_{cv} for the vertical ones. The anisotropy parameter h can then be defined as $h=I_{ch}/I_{cv}$. The horizontal junctions act as the coupling term between the vertical junctions. The dependence of a junction's current is sinusoidal with the phase; hence the interactions of the vertical junctions are anharmonic, with h serving as the measure of interaction strength. Figure 9 shows schematically two simple localized modes. The arrows indicate junctions that are rotating. All the other junctions librate at their equilibrium points. Type A breathers [Figure 9 (a)], are characterized by one vertical and two horizontal rotating junctions; type B breathers [Figure 9 (b)], are characterized by one vertical and four horizontal rotating junctions.

Since a rotating junction outputs a dc voltage, the breather solutions can easily be detected by measuring the average voltage of the different vertical and horizontal junctions. Figure 10 shows a typical result. We prepare the system in an initial condition with a breather located in the middle junction of the array (number 5) at I_a = 1.4 mA. We then decrease the applied current slowly. We start with the signature measurement of the breather: junction five is rotating at V_g while the neighboring junctions, V_4 and V_6, are at zero voltage. The horizontal junctions, V_{4T} and V_{5T}, have the expected value of $V_g/2$. As the current is decreased the breather persists until 0.8 mA, at which point the single-site breather destablizes, creating a two-site breather. We are currently investigating the properties of single-site and multi-site breathers in these Josephson lattices.

In addition to studying the discrete breathers themselves, we can also study how they interact with non-localized excitations such as vortices. We have fabricated arrays with paramaters that should allow for the simultaneous existence of a breather and a vortex. We have simulated numerically their interaction and find that the breather acts as a pinning center for the vortex motion. The pinned vortices become trapped in a potential well with an activation energy of about 22 Kelvin. We are currently working to verify these predictions experimentally.

Just as the discovery of soliton solutions led to the deeper understanding of non-linear systems and to subsequent applications outside the solid state community, it is hoped that the study and measurement of discrete breathers will add a new tool with which to further unlock mysteries of complex non-linear systems.

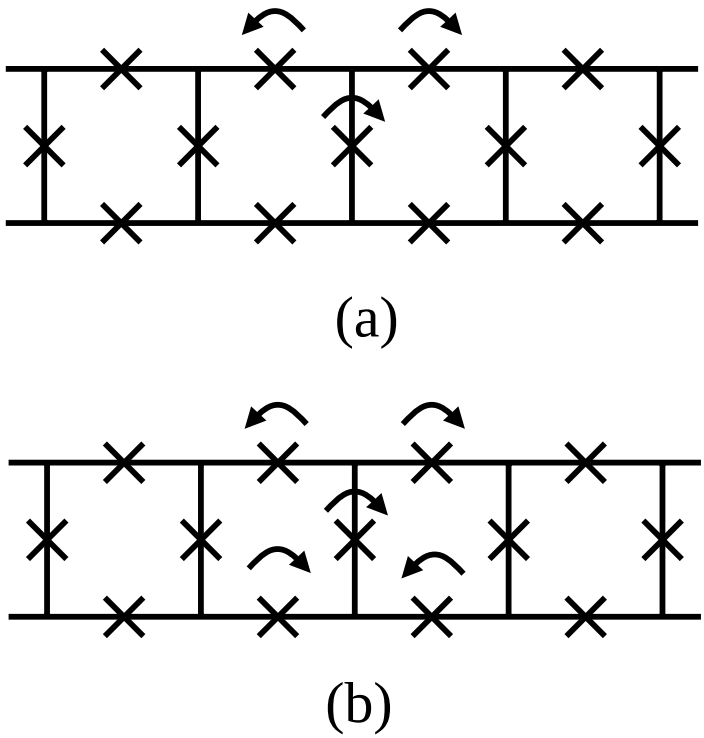

FIGURE 9. Schematic picture of breather solutions in ladder array: type A (a) and type B (b) breathers. Arrows are associated with rotating junctions.

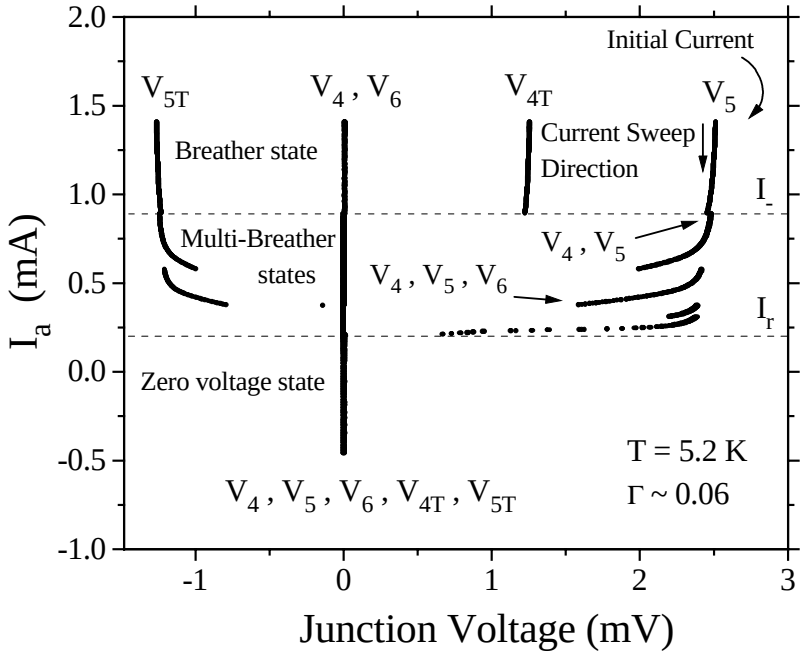

FIGURE 10. Measured time-averaged voltages of five junctions in the center of an array as the applied current is decreased. We have biased the ladder at 1.4 mA and excited a breather. Then the applied current is decreased.

Publications

Journal Articles, Published

Van der Wal, C.H., A.C.J. ter Haar, F.K. Wilhelm, R.N. Schouten, C.J.P.M. Harmans, T.P. Orlando, S. Lloyd, and J.E. Mooij. "Quantum Superposition of Macroscopic Persistent-Current States." *Science* 290: 773-777 (2000).

Trías, E., J.J. Mazo, and T.P. Orlando. "Discrete Breathers in Nonlinear Lattices: Experimental Detection in a Josephson Array." *Phys. Rev. Letts.* 84: 741-744 (2000).

Trías, E., J.J. Mazo, F. Falo, and T.P. Orlando. "Depinning of Kinks in a Josephson-junction Ratchet Array." *Phys. Rev. E* 61: 2257-2266 (2000).

Journal Articles, Accepted for Publication

Crankshaw, D.S., and T.P. Orlando. "Inductance Effects in the Persistent Current Qubit," *IEEE Trans. on Applied Superconductivity.* Forthcoming.

Crankshaw, D.S., E. Trías, and T.P. Orlando. "Tunable Power Output of a Parallel Array of Overdamped Josephson Junction." *IEEE Trans. on Applied Superconductivity.* Forthcoming.

Journal Article, Submitted for Publication

Berggren, K., D. Nakada, T.P. Orlando, E. Macedo, R. Slattery, and T. Weir. "An Integrated Superconductive Device Technology for Qubit Control," submitted for publication.

Book

Tian, L., L. Levitov, C.H. van der Wal, J.E. Mooij, T.P. Orlando, S. Lloyd, C.J.P.M. Harmans, and J.J. Mazo. "Decoherence of the Superconducting Persistent Current Qubit." *Quantum Mesoscopic Phenomena and Mesoscopic Devices in Microelectronics.* Eds. I.O. Kulik and R. Ellialtioğlu. Kluwer Academic Publishers, 2000.

Thesis

Trías, E. *Vortex Motion and Dynamical States in Josephson Arrays*. Ph.D. thesis. Department of Electrical Engineering and Computer Science, MIT, 2000.